SRI International

Final Report • 20 July 1998

THEORY OF ANION-SUBSTITUTED NITROGEN-BEARING III-V ALLOYS

Prepared by:

M. A. Berding, Senior Research Physicist
M. van Schilfgaarde, Senior Research Physicist
A. Sher, Associate Director
Applied Physical Sciences Laboratory

A. -B. Chen
Auburn University

SRI Project 1893
CDRL 0002AC

Prepared for:

Air Force Office of Scientific Research—AFOSR/NE
Directorate of Physics and Electronics
110 Duncan Avenue, Suite B115
Bolling Air Force Base, DC 20332-0001

Contract F49620-97-C-0026

Approved by:

Elizabeth J. Brackmann, Co-Director
Applied Physical Sciences Laboratory

REPORT DOCUMENTATION PAGE

Form Approved
OMB No. 0704-0188

1. AGENCY USE ONLY (Leave Blank)	2. REPORT DATE	3. REPORT TYPE AND DATES COVERED
	20 July 1998	Final Report

4. TITLE AND SUBTITLE

Theory of Anion-Substituted Nitrogen-Bearing III-V Alloys

5. FUNDING NUMBERS

Contract F49620-97-C-0026

6. AUTHORS

M. A. Berding, M. van Schilfgaarde, A. Sher, and A.-B. Chen

7. PERFORMING ORGANIZATION NAME(S) AND ADDRESS(ES)

SRI International
333 Ravenswood Avenue
Menlo Park, CA 94025-3493

8. PERFORMING ORGANIZATION REPORT NUMBER

1893FR

9. SPONSORING/MONITORING AGENCY NAME(S) AND ADDRESS(ES

Air Force Office of Scientific Research—AFOSR/NE
Directorate of Physics and Electronics
110 Duncan Avenue, Suite B115
Bolling Air Force Base, DC 20332-0001

10. SPONSORING/MONITORING AGENCY REPORT NUMBER

F49620-95-C-0004

11. SUPPLEMENTARY NOTES

None.

12a. DISTRIBUTION/AVAILABILITY STATEMENT

Distribution Statement A
Approved for Public Release.
Distribution is unlimited.

12b. DISTRIBUTION CODE

13. ABSTRACT *(Maximum 200 words)*

Because of the large bond-length mismatch between N and P or As, enormous internal strains strongly inhibit the miscibility of the latter into the anion lattice. This final report discusses the expected thermodynamic behavior of incorporation of P or As into the III-N lattice, by calculating the miscibility gaps in the regular solution model. The band states show some remarkable behavior when small amounts of phosphorous or arsenic are substituted for nitrogen. For example, when 1% As is substituted into GaN, a state is introduced into the gap at about 0.2 eV above the valence band edge (0.8 eV was found by Zunger group). When more than 4% arsenic is incorporated into GaN in an ordered array, the band gap closes. Calculations of the properties of random alloys predict smaller bowing than do the ordered alloy calculations. Hole lifetimes in $GaAs_{0.1}N_{0.9}$ are predicted to be quite low, of the order of 10^{-14} sec.

14. SUBJECT TERMS

Nitrides, alloys, semiconductors, wide band gap

15. NUMBER OF PAGES

21

16. PRICE CODE

17. SECURITY CLASSIFICATION OF REPORT	18. SECURITY CLASSIFICATION OF THIS PAGE	19. SECURITY CLASSIFICATION OF ABSTRACT	20. LIMITATION OF ABSTRACT
Unclassified	Unclassified	Unclassified	Unlimited

CONTENTS

LIST OF ILLUSTRATIONS

ABSTRACT

Because of the large bond-length mismatch between N and P or As, enormous internal strains strongly inhibit the miscibility of the latter into the anion lattice. This final report discusses the expected thermodynamic behavior of incorporation of P or As into the III-N lattice, by calculating the miscibility gaps in the regular solution model. The band states show some remarkable behavior when small amounts of phosphorous or arsenic are substituted for nitrogen. For example, when 1% As is substituted into GaN, a state is introduced into the gap at about 0.2 eV above the valence band edge (0.8 eV was found by Zunger group). When more than 4% arsenic is incorporated into GaN in an ordered array, the band gap closes. Calculations of the properties of random alloys predict smaller bowing than do the ordered alloy calculations. Hole lifetimes in $GaAs_{0.1}N_{0.9}$ are predicted to be quite low, of the order of 10^{-14} sec.

1 INTRODUCTION

This report concerns the theoretical investigation of the addition of As or P in GaN, or N in GaAs and GaP. Although the elements N, P, and As are in the same column, and should be chemically similar, the large size mismatch between N and P or As renders the substitution of one for the other very energetically unfavorable. Nevertheless, incorporation of up to 10% of N in GaAs has been reported.

A similar difficulty occurs in the substitution of C in Si. In this case—an idea which has been pursued for several years—the technological motivation stems from the possibility to simultaneously control the band offsets and lattice match in Si_xGe_{1-x} relative to Si with the addition of C. For the III-V compounds, the original purpose was, and continues to be "band-gap" engineering—that is, the tuning of the band gap (and band offsets) with the addition of N in Ga(P,As), or P or As in GaN.

Our Statement of Work proposed to investigate both the thermodynamics of the GaN_xP_{1-x} and GaN_xAs_{1-x} alloys for x near 0 and 1, and the changes in band structure the alloying introduces. In general, we have completed both of these tasks. The thermodynamic calculations show the heat of mixing to be very large, as expected. Because the lattice mismatch is approximately twice that of the $Ga_xIn_{1-x}N$ case, based on simple force-constant considerations we expect the heat of mixing to be about four times larger. This expectation was borne out by detailed first-principles calculations. Indeed, the results are so large that it is clear that highly nonequilibrium methods are essential to get concentrations of $x > 0.01$ or $x < 0.99$.

Investigation of the optical properties revealed some remarkable and unexpected behavior. The large mismatch in the anion p term values induces subbands to be split off from the valence band (which consists mostly of the anion p state). But these subbands are swept back into the valence bands as resonances when the lattice is allowed to completely relax. Calculations for the random alloy predict a smaller bowing than found for the ordered compounds.

2 THERMODYNAMICS

We employed the simplest theory for the calculation of phase diagram. (Since the experimental results are obtained using nonequilibrium techniques, there is little point in generating an elaborate equilibrium theory.) The "regular solution model" is derived from statistical theory in a zeroth-order approximation, and assumes a random configuration of atoms for the mixing energy and entropy. Moreover, one customarily makes the assumption that the mixing energy of an AB_xN_{1-x} alloy takes the form

$$H = xH_a + (1-x)H_b + \Omega x(1-x) \quad . \tag{1}$$

Then the excess free energy is

$$\begin{aligned} F &= H - TS \\ &= \Omega x(1-x) + kT\left[x \ln x + (1-x)\ln(1-x)\right] \quad . \end{aligned} \tag{2}$$

The justification for the functional form of H, Eq. (1), is grounded in the observation that for lattice-mismatched systems, Ω is dominated by strain, and to the extent a valence-force-field model or the bond-orbital approximation (Harrison, 1980) is valid, Eq. (1) is the correct functional form for H, in a random configuration of atoms. For the present purposes, we obtain Ω from total-energy calculations on supercells of the type A_{16} (BN_{15}), as an approximation to the dilute limit.

The regular-solution approximation itself can be justified on the following grounds. There are several techniques for calculating the critical temperature for miscibility gaps and spinodal curves versus x along the pseudobinary line of the ternary alloy phase diagrams. One technique developed recently features a statistical theory based on an analysis in the generalized quasichemical approximation (Chen and Sher, 1995). This analysis conveniently separates the problem into two types of contributions. The major contribution results in terms resembling the traditional regular solution model, with a mixing enthalpy parameter Ω interpreted somewhat differently. The second class of terms arises from correlation-induced short-range-order effects. Short-range order tends to extend the range of relaxed configurations around impurities, but usually makes only modest corrections to spinodal (or binodal) critical temperatures for most III-V alloys (though the effect in this case will be larger owing to large strain and the close proximity of the cations). However, even when the correlation correction is significant, it modifies the critical temperature by ~30 to 40%, not orders of magnitude. While correlation-

induced short range order has only a modest effect on the critical temperature, it has a substantial influence on phenomena sensitive to local surroundings — for example, dopant substitution energies.

There is another correction to the regular solution model that shifts the peak position of the miscibility and spinodal curves from the 50% concentration off to one side. These corrections are needed in a complete theory, and indeed, explicit total-energy calculations (not presented here) show that the asymmetry in the phase diagram is significant. Here the emphasis is on the principal characteristics of the phase diagrams — that is, those that help in understanding how to go about improving devices. Later, the complete theory formulated in Chen and Sher (1995, Chapter 4, Appendix A) can be implemented.

The heats of mixing for a random alloy were calculated with the full-potential linear muffin tin orbital (LMTO) method in the local density approximation (LDA), with a large basis including three sets of *spd* orbitals on the Ga site. This was sufficient to converge the total energy to within ~1 mRy of the exact LDA energy. An empirical tight-binding Hamiltonian was fit to the LDA binding curves, and this was used to relax the structures. The energetics were recalculated at the relaxed positions with the full-potential LMTO method, and additional relaxations were attempted around the tight-binding minimum to ensure the tight-binding relaxation was adequate. Thus, we are relatively confident that our result is the fully converged LDA with fully relaxed structures.

We obtain very large and positive heats of mixing, as expected. Without lattice relaxations, the energies are enormous—on the order of the bond strength. Lattice relaxations around the impurities were found to be large—approximately 10% of the bond length for nearest-neighbor relaxation, and the relaxations reduce the heat of mixing by about 75%, in accordance with simple estimates from force-constant models (Shih et al., 1985). Still, the remaining heats of mixing continue to be very large—approximately twice as large as that of In in GaN. In the regular solution model, the critical decomposition temperatures T_c are related to Ω by the simple expression $kT_c = \frac{\Omega}{2}$.

The alloy phase diagram is calculated from the usual common-tangent construction of the free energy. The critical temperatures are huge. T_c for GaN_xAs_{1-x} is seen from Figure 1 to be about 8000 K—something approaching the surface temperature of the sun! Since the LDA is expected to be reliable in generating Ω, Figure 1 shows that the experimental realization of 10% N in GaAs is achieved through a highly nonequilibrium process.

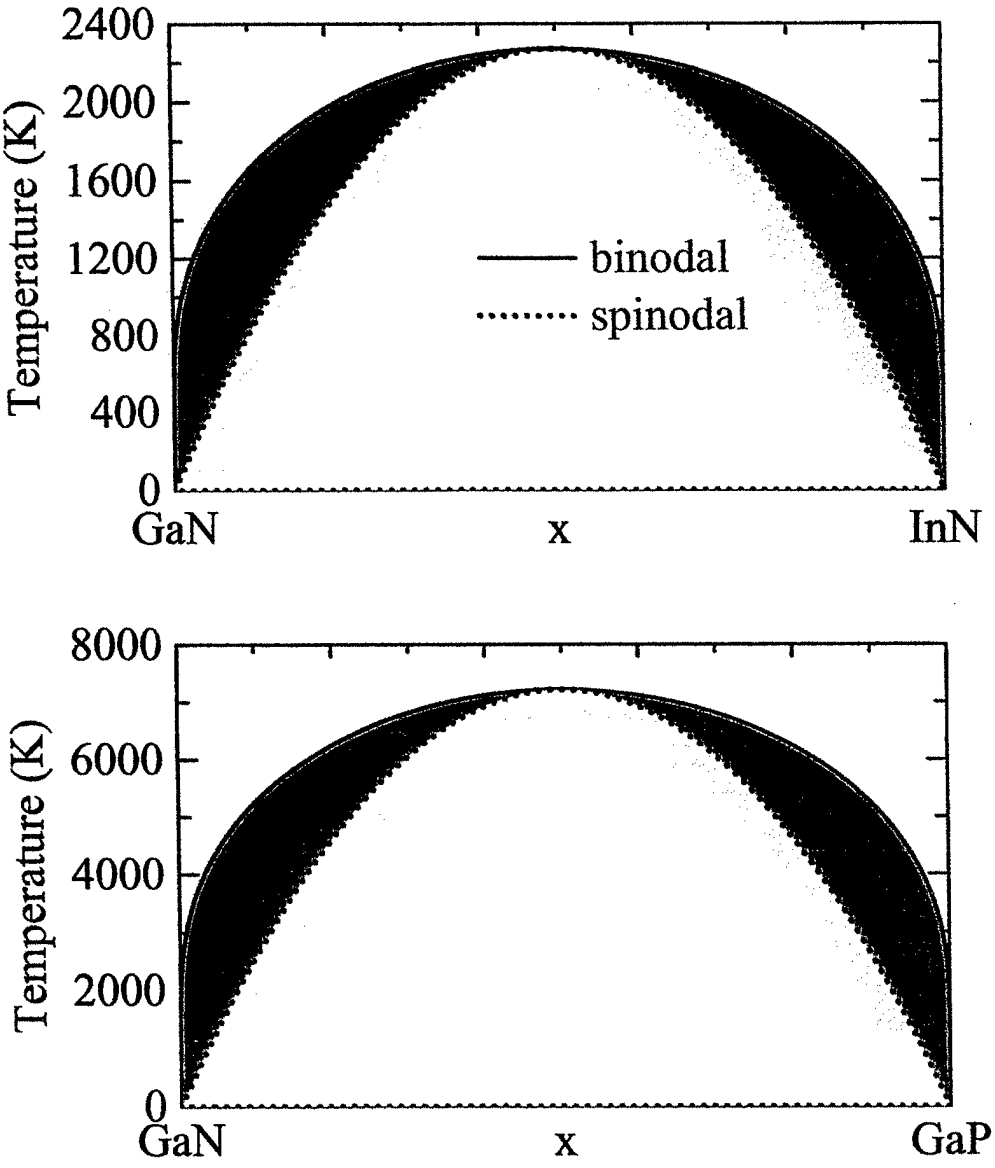

Figure 1: **Spinodal and binodal decomposition curves calculated in the regular solution model.** Top figure: $Ga_xIn_{1-x}N$. Bottom figure: GaN_xP_{1-x}.

3 OPTICAL PROPERTIES

We find remarkable and subtle changes in the energy bands when small amounts of N are mixed into GaAs or As or P into GaN. These changes are extremely sensitive to the alloy concentration x, the detailed configuration of the impurities, and the lattice relaxation around the impurities. For these calculations we employ the LMTO method in the atomic spheres approximation (ASA). This method is simpler and more approximate than the full-potential method, but can treat much larger systems. Even so, for optical properties it is usually true that the ASA generates bands quite close to more complete full-potential bands: We compared the ASA bands with full-potential bands for 32-atom cells, and found it to be the case for GaNP and GaNAs.

The changes in the band structure near the gap show remarkable behavior for $x \rightarrow 0$ and $x \rightarrow 1$, which as of this writing are not completely understood. Thus, this section reports on the situation as we now understand it.

Let us consider the dilute limit first. With the ASA, we can employ 216-atom supercells—for example, $Ga_{108}N_{107}P$, which corresponds to $x \approx 0.01$ or $x \approx 0.99$. The P impurities occupy a simple-cubic arrangement in the large supercell, and obviously do not correspond to a random arrangement of atoms. For this low concentration, it probably is not significant, because the concentration is sufficiently dilute to mimic an isolated impurity; but for higher concentrations, the geometrical arrangement is of crucial importance.

Figure 2 shows the total density of states (DOS) of 216-atom cells containing a single P or As in GaN, when the lattice relaxations are restricted to the nearest neighbors (NN) surrounding the impurity. There is a striking fairly sharp level emerging out of the top of the valence band edge. It is broadened into a narrow band because of interactions between impurities. For smaller cells (for example, $Ga_{64}N_{63}P$), the broadening is a little wider, and the center of gravity slightly shifted. Figure 3 shows the DOS resolved into partial contributions from the impurity and anions in shells successively farther from the impurity. There are several points of interest:

- The local character of the valence bands for P or As is much more heavily weighted toward the valence band top, as evidenced by the partial DOS relative to the bulk DOS. This is a consequence of the anion p state being much more shallow than the N p state.
- The level lies at $E_v + 0.18$ eV for P, and $E_v + 0.38$ eV for As. Very recently Zunger and coworkers (Bellaiche et al., 1997) also reported a sharp level, at $E_v + 0.5$ eV and $E_v + 0.75$ eV, respectively, using an empirical pseudopotential approach.

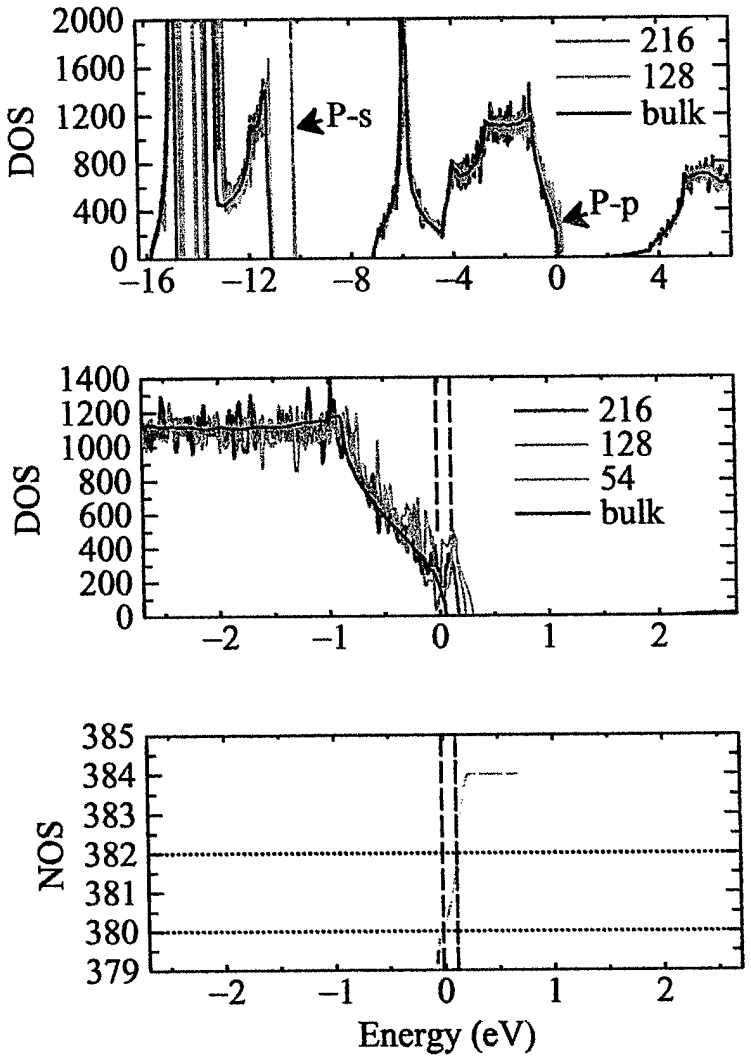

Figure 2: **Density of states of P in GaN of supercells of various sizes.** Relaxations were restricted to nearest neighbors. Top panel: DOS over entire valence band spectrum. A sharply localized P s state is indicated, as well as the P p valence subbands splitting off from the valence band maximum. Middle panel: the same DOS over a smaller energy range. Black line marks the bulk DOS. The split-off valence subbands above the valence band maximum of the bulk DOS are clearly seen, with the width broadening for smaller sized supercells. Bottom panel: integrated DOS for the 128-atom case. The black vertical lines mark two and four electrons, showing that above the bulk valence band maximum there are two levels. The system is neutral with 384 electrons, i.e., when the valence subbands are filled.

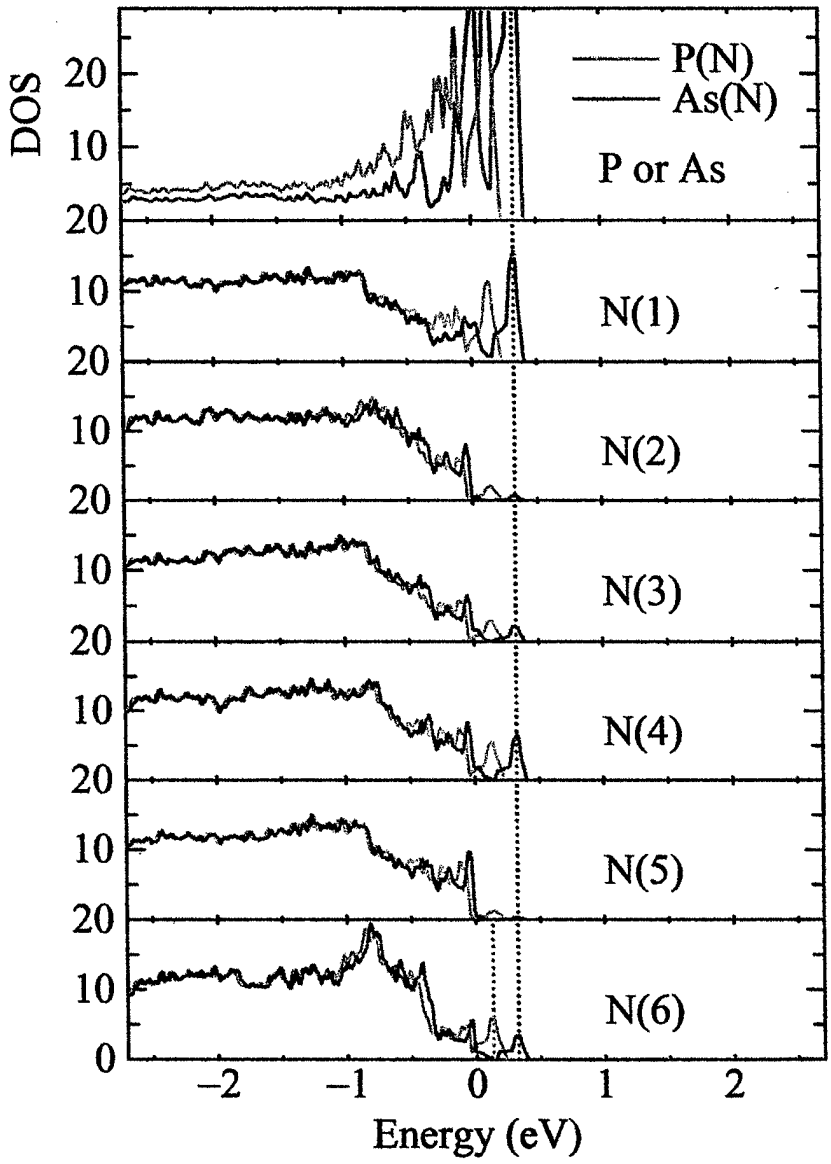

Figure 3: **Partial density of states of P and As in GaN, in a 216-atom supercell where only NN relaxations were included.** DOS correspond to the projection onto anion sites in shells successively farther from the defect. Red lines: DOS for P in GaN; blue lines: As in GaN. The bulk GaN valence band maximum is at about 0.

- There are actually two states, slightly split, carrying four electrons as determined by integrating the DOS over the width of the level.
- The partial DOS shows the eigenfunction is mostly centered around the impurity. Nevertheless, there is a significant weight extending well away from the impurity.

Thus we are led to the following conclusions when relaxations are restricted to NN. It might be argued that this approximately mimics the experimental situation where the alloy is grown epitaxially on a GaN substrate. There is a valence impurity subband extending slightly above the usual valence band maximum. It is mostly, but not completely localized, and thus can be characterized as a resonance or a weakly localized state such as P in Si. As regards its spatial extent, it resembles a shallow acceptor; but because the states are neutral when full, they behave with respect to their occupation as a very deep donor.

Remarkably, the situation changes dramatically when the entire lattice is allowed to relax, as is the case for a free-standing film. Now the localized subbands merge into the valence band. Figure 4 shows the corresponding partial DOS for the fully relaxed case. The figure shows that the P(As) subbands are swept into the valence band. Remarkably, the impurity introduces a long-range perturbation so that the DOS near the valence band maximum are significantly enhanced even in the anion shells farthest removed from the defect. That the P or As introduces a resonance that extends so far is perhaps not surprising, since states at the valence band maximum are extended. It is surprising, however, that near the impurity, there is an "antiresonance"—that is, the DOS are *reduced* relative to the bulk DOS, while far away the DOS are *enhanced.* A resonance in the conduction band is also evident from the figure.

Figure 5 shows the average change in electrostatic potential relative to that of the bulk DOS. It is evident that this change extends well away from the impurity; moreover, it evolves to a value approximately 0.2 eV larger than the bulk. Since the bulk DOS was shifted by only 0.1 eV to align the valence band maximum, this signifies that there remains an additional shift of 0.1 eV. Thus, we can estimate that the valence band offset of this material relative to that of bulk GaN is 0.1 eV. It is clear that this offset is induced by the strain field, since there is no such offset in the NN-relaxed case (Figure 2).

When they allow complete relaxation, Bellaiche et al., (1997) report a finding similar to our NN relaxed case, but find only a single level, much deeper in the gap. We attribute the discrepancy with our results to their use of an empirical pseudopotential, which was fit to LDA bands for higher concentrations. It is likely that the dielectric screening is not properly accounted for in Zunger's empirical approach.

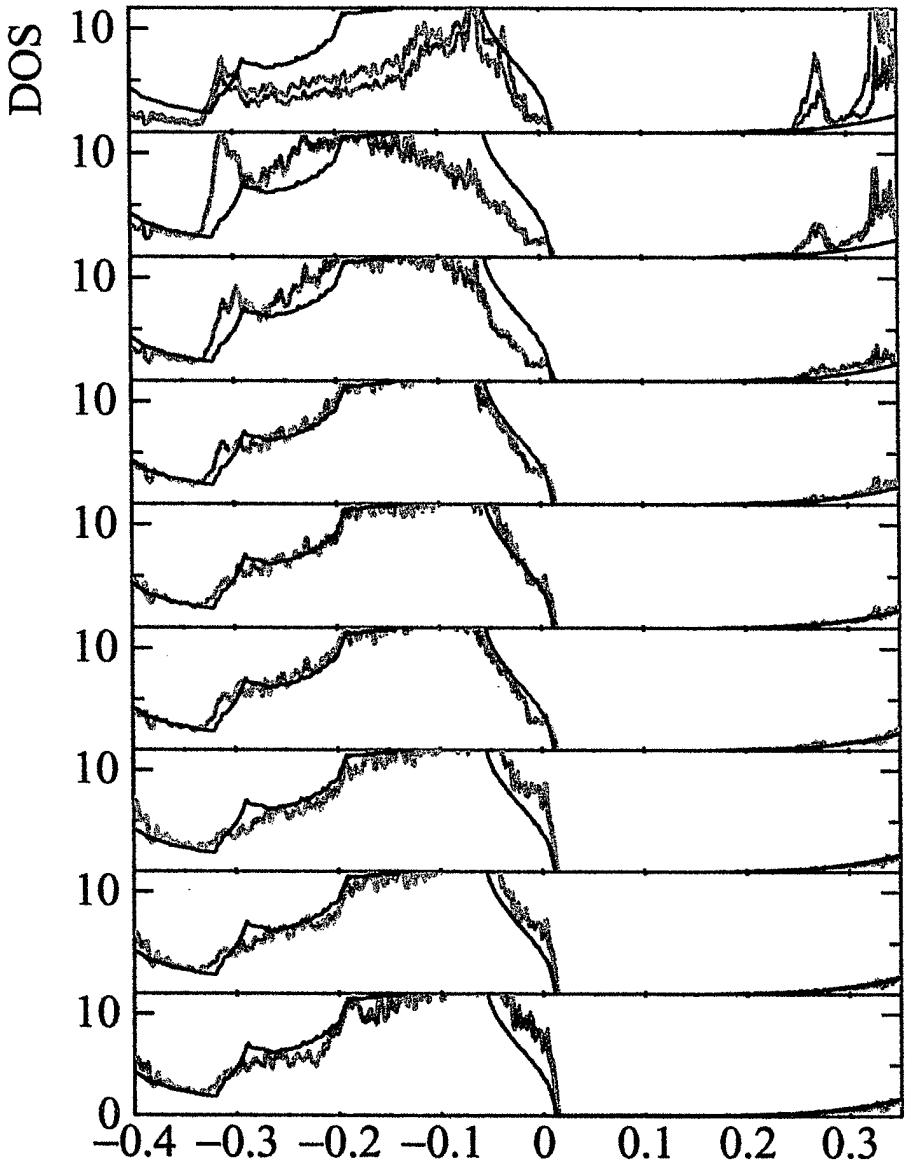

Figure 4: **Partial density of states of P and As in GaN, in a fully relaxed 216-atom supercell.** DOS correspond to the projection onto anion sites in shells successively farther from the defect. Red lines: DOS for P in GaN; green lines: As in GaN; blue lines: bulk GaN DOS. The blue DOS was shifted by 0.1 eV to align the valence band maxima. The calculation shows there is a band offset of the defect material relative to the bulk, as discussed in the text.

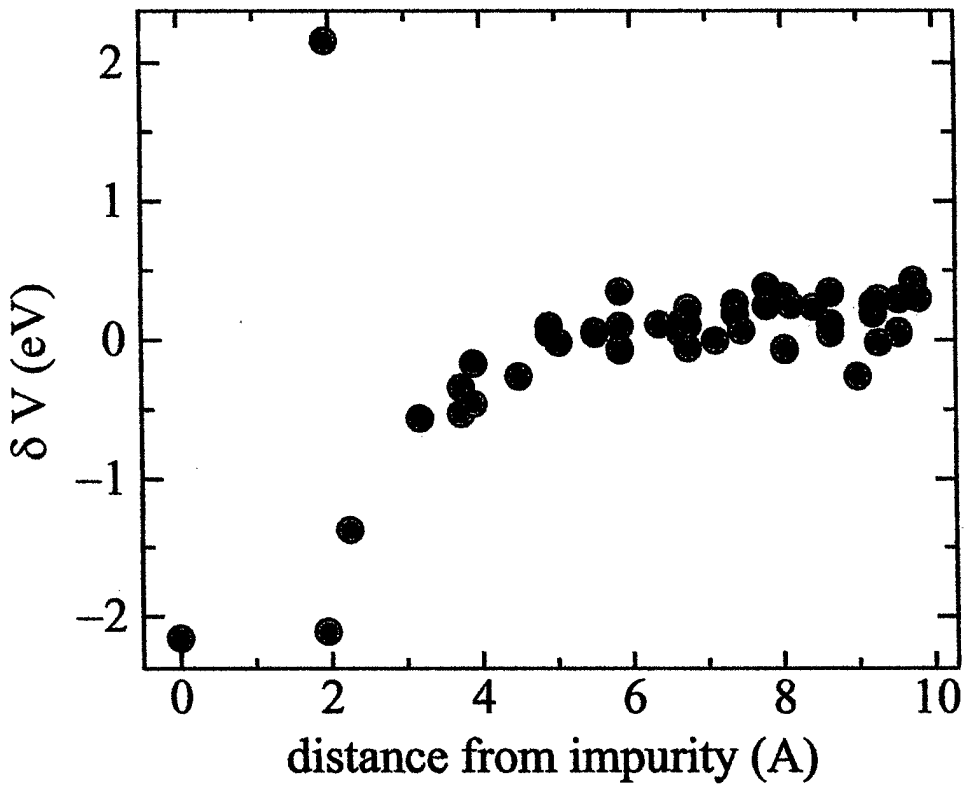

Figure 5: **Average electrostatic potential shifts relative to bulk values as a function of distance from P impurity.** These are taken from the fully relaxed 216-atom supercell. The shift is relatively long ranged, converging an asymptote of ~0.2 eV.

4 RANDOM ALLOY CALCULATIONS

Recently Bellaiche, Wei, and Zunger (BWZ) (Bellaiche et al., 1997) have studied the band gap states of $GaAs_{1-x}N_x$. In their work, fitted pseudopotentials and a constrained plane-wave set were employed in large supercell calculations to obtain the highest valence band and lowest conduction band energies (at $\mathbf{k} = 0$) in several random configurations for a given alloy concentration. They have found several interesting results: large bowing parameters, strong variation of bowing parameters with concentration, and the localization of valence-top states in the dilute As or P cases. They have also shown that, when the alloys structures are conformed to the substrates, the calculated gaps agreed reasonably with the measured gaps for several alloys with low N concentrations. It is thus interesting to see if the same qualitative physics can be obtained from the completely different approach that we have been using—the average Green function approach based on the molecular coherent potential approximation (MCPA) and a hybrid pseudopotential tight binding (HPTB) band scheme. We note that the average Green function can yield the whole alloy energy spectra, not just the band edges. It also provides the important information about the lifetime of Bloch states caused by alloy disorder.

The band structures based on HPTB are obtained in a similar manner as that described in Chen and Sher (1995), with the input band structures deduced from a combination of the available theoretical and experimental (very little) results (van Schilfgaarde et al., 1997). Figures 6 through 8 show the band structures constructed for AlN, GaN, and InN, respectively.

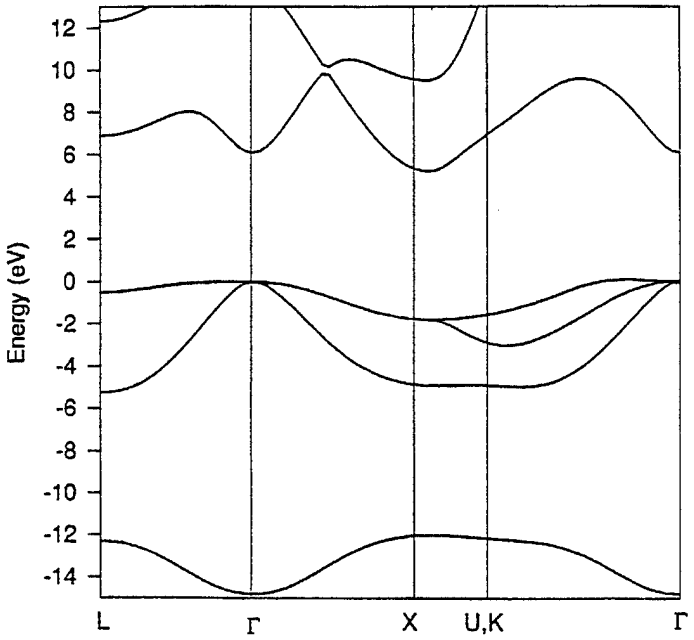

Figure 6 BAND STRUCTURE OF ZINC BLENDE AIN

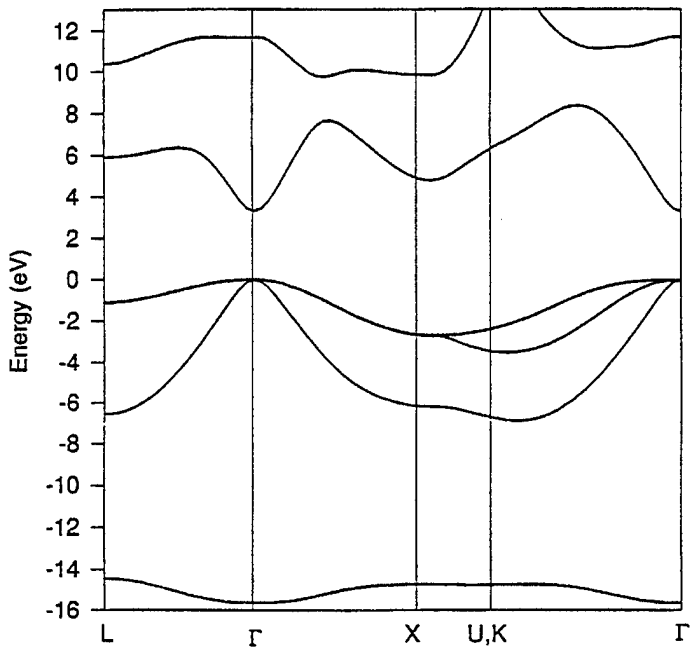

Figure 7 BAND STRUCTURE OF ZINC BLENDE GaN

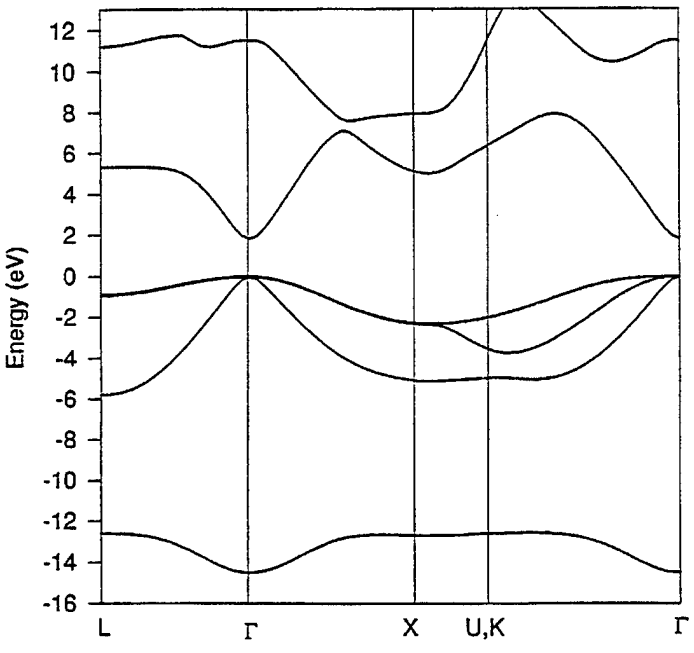

Figure 8 BAND STRUCTURE OF ZINC BLENDE InN

The band structure parameters for the nitride compounds are then used along with those of the other III-V compounds obtained in Chen and Sher (1995) in the MCPA calculation. In this approach, a molecular unit consists of eight hybrid orbitals along the four tetrahedral bonds surrounding each alloying atom (the anions in the present case). The differences in the intra-molecular TB matrix elements between the two different molecular units are the alloy scattering potentials. The fluctuations in these matrix elements have two origins: the difference in the atomic term values and the first-neighbor interactions which depend on the pairs of atoms considered and the bond lengths governed by a bimodal bond-length distribution in the alloy. Here we focus on GaAsN alloys, for which the scattering parameters are given in Table 1. Similar results for other anion-substituted nitride alloys can also be generated if needed.

Table 1

ALLOY DISORDERED PARAMETERS AS DEFINED IN EQ. (5.11.2) IN CHEN AND SHER (1995) FOR $GaAs_{1-x}N_x$ at $x = 0.5$

Representation	δ (eV)	Δ (eV)
Γ_6	–5.593	0.257
Γ_7	–2.856	–0.153
Γ_8	–3.212	–0.2153

The scattering parameters shown in Table 1 indicate that these alloys are strong-scattering alloys as compared with all the cases studied in Chen and Sher (1995). While the atomic t-matrix approximation (ATA) and CPA gave virtually the same results for all the III-V alloys studied in Chen and Sher (1995) (because alloy scattering is weak), ATA is not adequate for the present study. Therefore, a complete MCPA calculation, which is computationally much more expensive than ATA, has to be carried out.

Figure 9 shows the plots of spectral density of states in the energy range around the band gap for $GaAs_{1-x}$ at $\mathbf{k} = (0,0,0)$ for $x = 0.1$, 0.5, and 0.9. The arrows indicate the delta-functions correspond to the band structures in the virtual crystal approximation (VCA). Since the spin-orbital coupling is included, the three VCA energies from lower to higher energies correspond to Γ_7 (2-fold), Γ_8 (4-fold), and Γ_6 (2-fold) states, respectively. While the Γ_6 spectral DOS remains reasonably sharp, the Γ_7 and Γ_8 spectral DOS are broadened substantially. We note that at the bottom panel the spin-orbit splitting is very small, and the two peaks are not the Γ_7 and Γ_8, respectively; they represent the split-band caused by the strong alloy scattering. This split-band limit is also evident from the bottom panel in Figure 10 where total density of states is plotted.

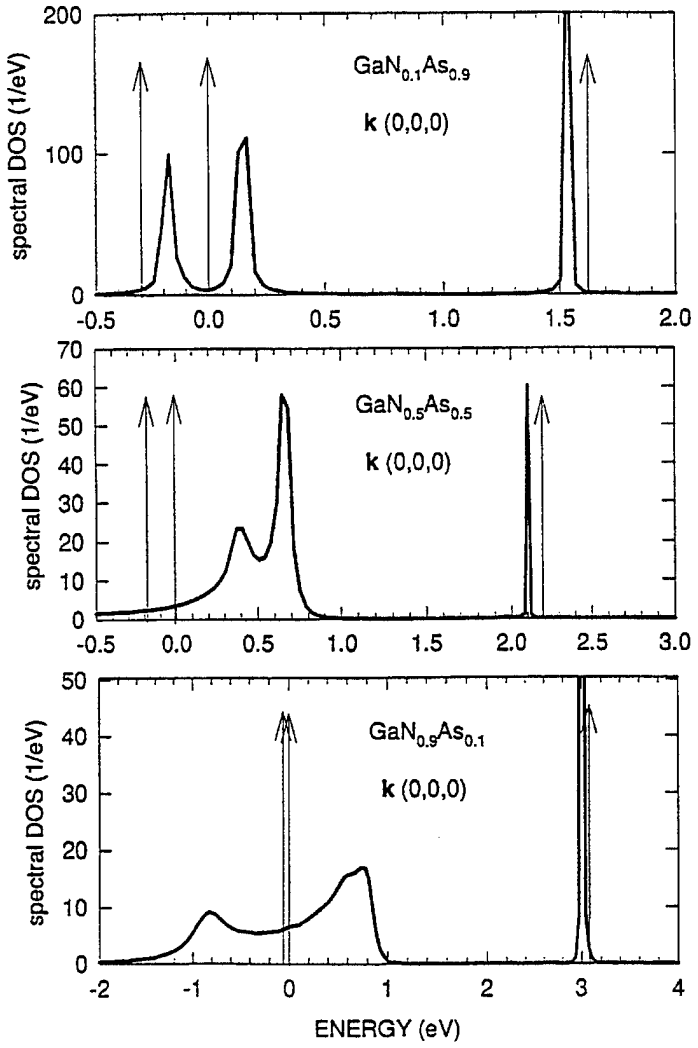

Figure 9 SPECTRAL DENSITY OF STATES AT k = (0,0,0) FOR SEVERAL GaNAs ALLOYS

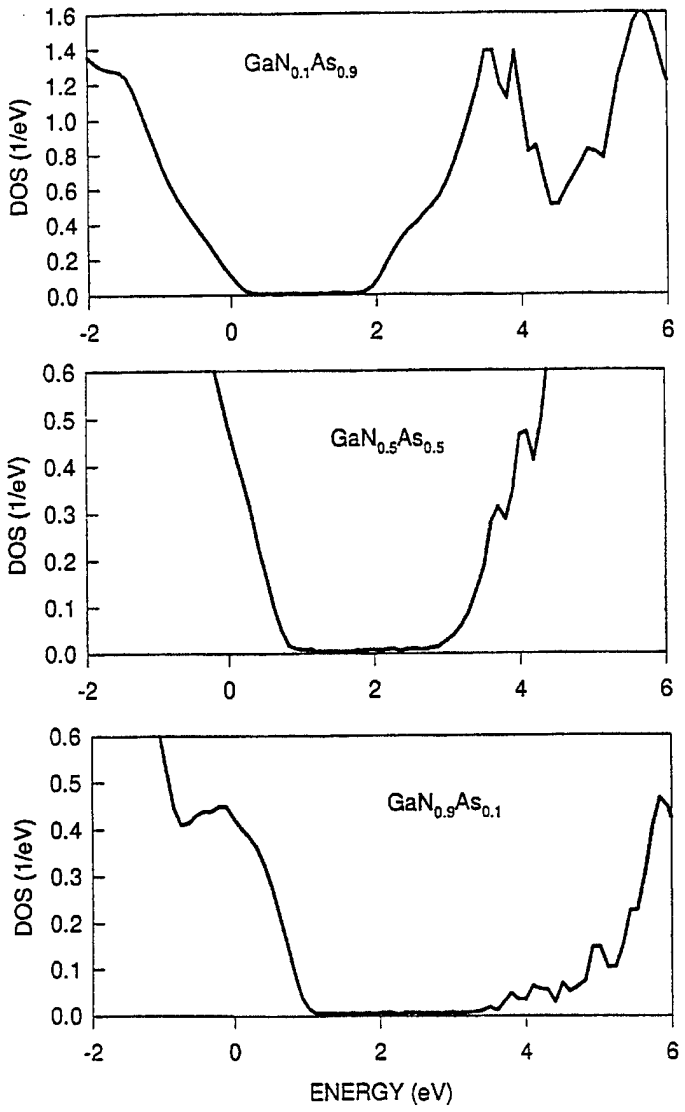

Figure 10 DENSITY OF STATES FOR SEVERAL GaNAs ALLOYS

Given the broadened spectral DOS, it is not unambiguous to define the band gap. There are two possible choices within the present framework: the energy separation between the peaks, or that between the two edges of the Γ_7 and Γ_8 spectral DOS. Neither choice is unique. Also, there is no unique way to define the edges. The bottom line marked by "edge" in Figure 11 is the separation between the edges chosen at the energies where the spectral DOS has a value of 0.5 of scale used in Figure 10. This is about the uncertainty in the magnitude of the calculated spectral DOS. Also plotted in Figure 11 are the energy separation between the two peaks (the curve marked by "peak") and the band gap in VCA. The several experimental gaps available all lie between the two lower curves but closer to the lowest one.

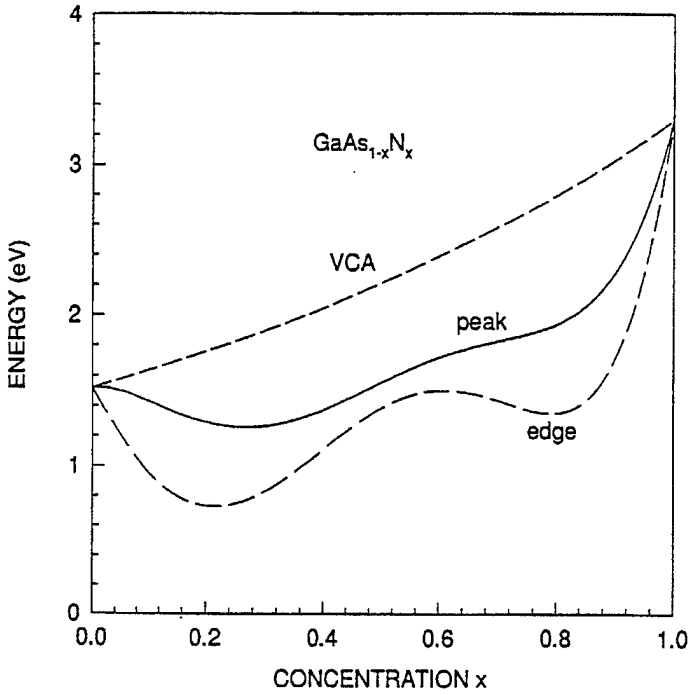

Figure 11 BAND GAP FOR GaAsN ALLOYS

From the physics point of view, this is an interesting case because it is the first pseudo-binary semiconductor alloy that has an alloy scattering potential strongly influencing the band-edge states, particularly the valence band top. This broadening in the spectral DOS implies that hole mobility is severely limited. Even though the broadening ($\approx$ 0.1 eV, corresponding to 10^{-14} sec in lifetime) in the spectral DOS for the conduction band edge is not as great as seen from Figure 9, it is significantly larger than other III-V alloys. Thus, in terms of normal semiconductor application, this alloy is a poor one, not only with a limited mobility, but also with a great difficulty of mixing (because of large lattice mismatch). However, there may be new applications associated with the new features in the electronic structures such as band tails and large variation of band gap and mobility with concentration and temperature.

We note that the present MCPA study and BWZ's work are not adequate for the study of the band tail and the mobility edge. The CPA only effectively treats the extended states while BWZ only probes one or two states, and it is difficult to exhaust enough configurations to be statistically significant. Both studies also have not explicitly included the d-states in the calculation, which may alter some of the above results.

5 SUMMARY

For thermodynamics properties, we found enormously large heats of formation. Indeed, based on these data, it is quite surprising that up to 10% N has been reported to be incorporated into GaAs, and suggests that probably much of the N is not going in substitutionally. In any case, it seems clear that growth results from a highly nonequilibrium process.

As regards the band structure, some remarkable behavior is found, even with less than 1% incorporation of P or As. We find already at the 1% a reduction in the gap of ~0.1 eV, indicating a large bowing in the dilute limit. The valence band maximum, which consists mostly of the anion *p* orbitals, splits into subbands; these subbands dissolve into resonances when the lattice around the impurity is allowed to relax. (It may be true that the unrelaxed case corresponds approximately to the experimental situation where the film is constrained to be lattice matched to the bulk GaN. If these subbands are present, they should strongly enhance excitonic effects, and thus laser grain.) In any case, these states propagate well away from the impurity, and thus resemble a resonance that is somewhere between a hydrogenic defect and a propagating state one usually finds at the band edge in an alloy. One important consequence of this is that the effective mass is probably increased significantly.

6 REFERENCES

Bellaiche, L., S.-H. Wei, and A. Zunger, "Band gaps of GaPN and GaAsN alloys," *Appl. Phys. Lett.* **70,** 3558 (1997).

Chen, A.-B and A. Sher, *Semiconductor Allous: Physics and Materials Engineering* (Plenum, New York, 1995).

Harrison, W. A., *Electronic Structure and the Properties of Solids* (Freeman, San Francisco, California, 1980).

Shih, C. K., W. E. Spicer, W. A. Harrison, and A. Sher, *Phys. Rev.* **B31,** 1139 (1985).

van Schilfgaarde, M., A. Sher, and A.-B. Chen, *J. Crys. Growth* **178,** 8 (1997).

20 July 1998

Defense Technical Information Center/OCP
8725 John J. Kingman Road, Suite 0944
Fort Belvoir, VA 22060-6217

Subject: Final Report

Reference: Contract F49620-97-C-0026
(SRI Project ESU-1893)

SRI International is pleased to submit two (2) copies of our Final Report entitled "Theory of Anion-Substituted Nitrogen-Bearing III-V Alloys." This report has been prepared in accordance with the requirements of CDRL 0002AA of the referenced contract.

If you have any questions, do not hesitate to contact me at (650) 859-4424 or via email at baxter@sri.com.

Sincerely,

Margaret Baxter
Senior Contract Administrator

Enclosures

SRI International
333 Ravenswood Ave. • Menlo Park, CA 94025 • (415) 326-6200 • TWX: 910-373-2046 • Telex: 334486